Dynamic Molecular Oxygen Accessibility to a Buried Mn^{2+} Protein Site: A High-Field EPR Experiment

Tatyana I. Smirnova* and Alex I. Smirnov

North Carolina State University, Department of Chemistry, 2620 Yarbrough Drive, Raleigh, North Carolina 27695-8204

Received: April 10, 2003

A high-field (W-band, 3.35 T, 95 GHz) electron paramagnetic resonance (EPR) experiment to measure dynamic molecular oxygen accessibility to manganese(II) ions in liquids is described. The method is based on the direct observation of magnetic interactions between molecular oxygen and the manganese(II) ion in solution. The effect is observed as a Lorentzian broadening of the EPR line. The observation of this effect is facilitated by narrowing the manganese(II) EPR signal at high magnetic field and utilizing elevated oxygen pressures of up to 3 atm. The magnitude of the broadening effect is dependent on both the oxygen permeability of the solvent and the coordination of the manganese(II) ion and is independent of the frequency of the EPR experiment. The latter indicates that Heisenberg spin exchange between the electronic spins of oxygen and manganese(II) during bimolecular collisions is the likely broadening mechanism. The method can be also used to study dynamic molecular oxygen accessibility to manganese(II) sites in biological macromolecules, as demonstrated by an example of a buried site in Concanavalin A lectin. It was found that the oxygen accessibility of this site is significantly smaller (by a factor of 4) than that of an aqua ion and is recovered upon denaturing of the protein.

Introduction

Molecular accessibility of protein residues and especially buried functional sites is of fundamental importance to understanding the mechanisms of molecular recognition, function, and signaling. Static X-ray crystallographic structures often offer little or no clues about the accessibility of the buried sites, because of the unknown magnitude of protein structural fluctuations. Accessibility of buried paramagnetic metal ion sites to small paramagnetic molecules such as O_2 and NO are of fundamental importance for understanding the mechanisms of oxygen transport, redox processes that occur at the metal sites, and nitric oxide signaling. One point of view is that, in tightly packed folded proteins, very little molecular oxygen (O_2) diffuses through the material. On the other hand, fluctuations in protein side chains may be responsible for passing small molecules such as O_2 and nitric oxide to the myoglobin binding site with little or no barrier.[1]

Currently, O_2 accessibility experiments are performed using fluorescence quenching,[2,3] NMR,[4−6] and site-directed spin-labeling electron paramagnetic resonance (EPR).[7−11] It has been recognized that, in these methods, molecular oxygen serves as a very unique biophysical probe that is particularly suitable for microheterogeneous biopolymers, because of its small size and appropriate level of hydrophobicity.[12] These properties allow an O_2 to enter even the smallest vacant pockets that are transiently formed in proteins or membranes.[10−13] The EPR method is based on the interaction of a O_2 molecule, which acts as a probe, with a nitroxide radical, which is used as a reporter. The interaction results in the shortening of both T_1 and T_2 electronic relaxation times of the radicals. In continuous-wave (CW) EPR, this T_2 effect is observed as a Lorentzian line broadening that is proportional to the oxygen permeability of the solvent. The effect of oxygen on nitroxide EPR spectra became the foundation of EPR oximetry, which has found numerous biochemical and biophysical applications.[12,14−18] It also led to remarkable site-directed spin labeling experiments for elucidating protein structures and transmembrane protein locations, based on the oxygen accessibility of protein residues that were selectively labeled with nitroxides.[19] In comparison to NMR and fluorescence quenching experiments, the EPR method has perhaps the most suitable time scale, because the relaxation time of a typical nitroxide attached to a protein side chain is approximately a few nanoseconds. This coincides with the correlation time of typical side chain fluctuations. The disadvantage of the spin-labeling EPR approach is that it requires chemical modification of the site of interest. Neither fluorescence quenching, NMR, nor site-directed spin-labeling EPR methods are capable of measuring the O_2 accessibility directly at the metal ion center.

Here, we describe initial experiments to directly observe dynamic magnetic interactions between a Mn^{2+} ion and molecular oxygen (O_2) in solutions from linewidth effects in high-field (3.4 T, 95 GHz, W-band) EPR spectra. The dynamic effect of O_2 on the EPR spectra of paramagnetic metals is, to the best of our knowledge, not documented in the literature, although static broadening of rigid limit (at a temperature of 77 K) Cu^{2+} X-band EPR spectra in zeolites by absorbed O_2 was reported previously.[20]

At physiological temperatures, the electronic relaxation of many paramagnetic metal ions is so short that no EPR is observed. Even when the EPR of paramagnetic metal ions in solution is detected, the lines are too broad and the electronic relaxation is too short for CW saturation or pulse saturation recovery EPR experiments. We have chosen the Mn^{2+} ion for our experiments for several reasons. First, the Mn^{2+} ion gives

* Author to whom correspondence should be addressed. E-mail: Tatyana_Smirnova@ncsu.edu.

10.1021/jp0349637 CCC: $25.00
Published on Web 07/01/2003

the narrowest CW EPR linewidth for solution spectra among the other transition-metal ions, which facilitates the observation of linewidth changes. Second, the electronic spins of the Mn^{2+} ion are less shielded than, for example, the Gd^{3+} ion; thus, one could expect stronger magnetic interactions in the course of molecular collisions with oxygen. Finally, but not last, the Mn^{2+} ion has an important role in enzyme regulation.[21] The EPR frequency of 95 GHz was chosen to facilitate observation of the oxygen effect, because the Mn^{2+} EPR linewidth narrows substantially with increasing magnetic field.

Experimental Section

To perform re-equilibration of aqueous solutions with different gases inside a W-band EPR cavity, we have adapted a degassing method that was previously described for X-band spectrometers,[12,18,22] but microbore poly(tetrafluoroethylene) tubing (inner diameter of 0.152 ± 0.025 mm; wall thickness of 0.127 ± 0.025 mm; Cole−Parmer, Vernon Hills, IL) was used. The capillary was positioned through the center of a cylindrical W-band TE_{012} resonator so that the ends remained outside the cavity, and a gas flow with the desired oxygen content was directed to the cryostat through the waveguide directly to the sample. In a typical experiment, a solution was initially equilibrated with nitrogen (or helium), and then EPR spectra were acquired continuously while switching the gas to pure oxygen. At room temperature, re-equilibration of an aqueous solution drawn inside such a capillary occurred with a time constant of $t_{1/2} \approx 4-6$ min. This value is acceptable for most experiments. Elevated oxygen pressure experiments were performed by pressurizing the entire variable temperature cryostat (Oxford Instruments, Ltd., Concord, MA) that contained the W-band probe head with a desired compressed gas.

To separate the oxygen broadening effect from the intrinsic linewidth of the Mn^{2+} ion, we have applied a one-linewidth-parameter fitting model that was previously developed by Smirnov and Belford for fitting inhomogeneously broadened EPR spectra.[18,23]

This model is based on simulating CW EPR spectra with convolution eq 1, in which $F_0(B')$ is the spectrum taken in the absence of oxygen and $F(B)$ is the spectrum taken in the presence of oxygen; $m(B)$ is the Lorentzian broadening, measured as the $\delta(\Delta B_L{}^{p-p})$ peak-to-peak line width.

$$F(B) = \int_{-\infty}^{+\infty} F_0(B')m(B - B')\,dB' \qquad (1)$$

We have shown previously that this model is applicable to the measurement of oxygen permeability from nitroxide membrane probes in phospholipid bilayers at temperatures corresponding to ripple and fluid bilayer phases.[18]

Concanavalin A lectin, from *Canavalia ensiformis* (hereafter referenced as Con-A), and Mn^{2+} salts were purchased from Sigma−Aldrich (St. Louis, MO) and were used as received. Perdeuterated nitroxide Tempone (PDT, 4-oxo-2,2,6,6-tetramethylpiperidine-d_{16}-1-oxyl) was purchased from Cambridge Isotope Laboratories (Andover, MA).

Results and Discussions

It was expected that the oxygen effect on Mn^{2+} W-band EPR spectra would be small. For example, for nitroxides, the broadening in oxygen versus nitrogen-saturated aqueous solutions is 0.63−0.73 G,[22] which is readily observed for 0.2−1.0 G intrinsic linewidths. One could expect that the electronic spins of the Mn^{2+} ion are shielded somewhat better than those for nitroxides, resulting in lesser broadening. Also, this effect should be difficult to observe, because of the larger intrinsic linewidth of the Mn^{2+} ion (ca. 7−15 G, depending on the coordination, at W-band) versus free radicals.

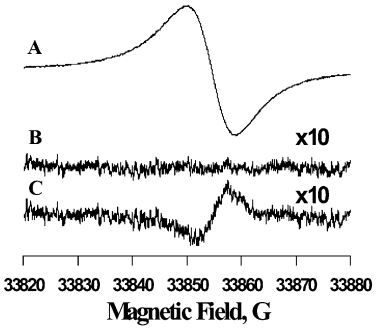

Figure 1. Oxygen effect on the $m_I = {}^1/_2$ hyperfine component of the 95 GHz EPR signal from a 2.5 mM aqueous solution of MnEDTA: (A) oxygen-equilibrated solution; (B) 10-fold amplified residual of the fit using eq 1; and (C) 10-fold amplified residual using eq 1 but assuming that there is no change in the linewidth.

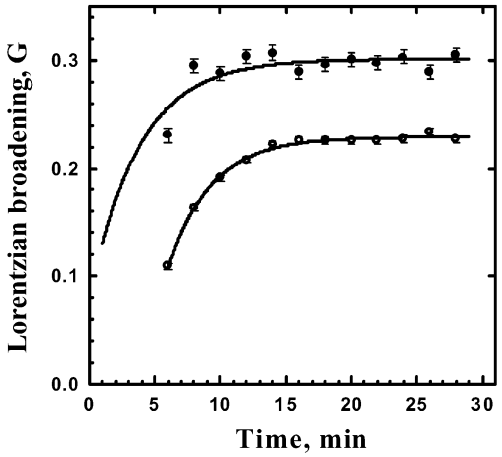

Figure 2. Kinetics of Lorentzian broadening upon re-equilibration of nitrogen equilibrated solutions of (○) $Mn(NO_3)_2$ and (●) MnEDTA with oxygen.

Experiments with several Mn^{2+} salts and a MnEDTA complex showed that the model of Lorentzian broadening fits the experimental data exceptionally well. Figure 1A shows the $m_I = {}^1/_2$ component of the 95 GHz EPR spectrum of oxygen-equilibrated 2.5 mM aqueous solution of MnEDTA; Figure 1B is the 10-fold amplified residual of the fit using eq 1, and Figure 1C is the 10-fold amplified residual of the fit using eq 1 but assuming that there is no change in the linewidth (i.e., the position, signal intensity, baseline line, and dispersion contribution to the spectrum were allowed to vary, but not the linewidth). The residual shows that our model is appropriate for fitting of the experimental data. The oxygen broadening determined from this fit is 310 ± 30 mG. As a control, we have observed the narrowing of Mn^{2+} spectra to the same initial width upon re-equilibration of the initially oxygenated sample with helium.

The least-squares simulations were performed in automatic mode for all sequential EPR spectra collected upon the oxygenation or deoxygenation of solutions. Figure 2 shows the kinetics of oxygen broadening that was observed for $Mn(NO_3)_2$ and MnEDTA at the W-band (please note that the time scale shown has a different starting point for switching the bathing gas to O_2 in these two experiments). The curves illustrate that, despite the rather small magnitude of the effect, our method produced repeatable and consistent results: i.e., the curves are well approximated by first-order kinetics, which is a good model

TABLE 1: Oxygen Broadening of EPR Spectra from Aqueous Solutions of Mn^{2+} Compounds and a Nitroxide Radical

	Broadening, mG	
compound	from 9.5 GHz EPR	from 95 GHz EPR
MnEDTA		300 ± 30
$Mn(NO_3)_2$	170 ± 70	230 ± 30
nitroxide PDT	650 ± 10	655 ± 30

for the final stages of oxygen diffusion to the limited volume of a gas-permeable capillary.[24] By fitting these curves to first-order kinetics and averaging the results of multiple measurements, a greater accuracy of oxygen-induced broadening is achieved. Comparative data of oxygen broadening effects for the aqua Mn^{2+} ion and MnEDTA are summarized in Table 1.

The table shows that the oxygen effect on Mn^{2+} W-band EPR spectra is rather small, as expected. By analyzing the kinetics of oxygen-induced broadening, we have estimated the errors in the extracted oxygen broadening to be <10 mG at 68% confidence intervals for all data sets. Nevertheless, for the reported data, we have chosen conservative ±30 mG error intervals, to reflect the minimum 30-mG magnetic step of the digital power supply utilized in these experiments.

We also attempted the same measurements at the X-band. The results of least-squares fitting gave a similar value for the oxygen broadening effect that was observed for $Mn(NO_3)_2$ at W-band but with much larger error (170 ± 70 mg). However, the determination of oxygen broadening from X-band spectra is less reliable. It was also found that, when the intrinsic linewidth is large, as for the Mn^{2+} ion at the X-band (ca. >24 G), the changes in the baseline term and the linewidth become correlated, which could be a potential source of even larger errors. To demonstrate that the oxygen-induced Mn^{2+} spectral broadening is affected by the oxygen permeability coefficient of the solvent, we have conducted W-band EPR experiments with Mn^{2+} salt solutions in 80% v/v ethanol−water mixtures. Oxygen broadening in an EPR spectrum from $Mn(NO_3)_2$ in an 80% v/v ethanol−water mixture, compared to that of pure aqueous solution, increases by a factor of 3.6, as expected, because of higher oxygen permeability of the mixed solvent, compared to pure water.

To fully utilize the oxygen relaxation enhancement for characterization of metal binding sites in more-complex systems, it is necessary to amplify the magnitude of this effect. Increasing in the oxygen partial pressure up to a few atmospheres should magnify the effect and make measurements more reliable. Although routine EPR experiments with elevated gas pressure require a specialized setup, we have attempted the first demonstration by pressurizing the entire variable temperature cryostat that contained the W-band EPR probe head. The plot of circular symbols in Figure 3shows the dependence of oxygen broadening for 2 mM aqueous $MnCl_2$ as a function of oxygen pressure. The dependence is linear (in this pressure range, the oxygen solubility closely follows Henry's law), illustrating that the effect is proportional to oxygen permeability. Figure 3 also illustrates that even moderately elevated pressures of ca. 3 atm can make the broadening effect easily detectable. No changes in the Mn^{2+} spectra were observed in control experiments that were conducted in a helium atmosphere at pressures up to 3 atm.

Room-temperature Mn^{2+} HF EPR spectra are easily observed for ions that are bound to proteins and RNAs, and the oxygen broadening method might be useful to characterize the transient environment of these ions. As a first step to demonstrating this effect for the characterization of oxygen accessibility at a

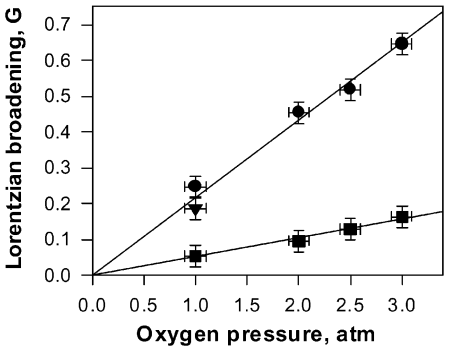

Figure 3. Oxygen-induced Lorentzian broadening as a function of oxygen pressure: (●) 2 mM aqueous solution of $MnCl_2$, (■) 0.75 mM solution of Con-A in pH 6.4 HEPES, and (▼) 0.75 mM solution of denatured Con-A in 4 M GndHCl.

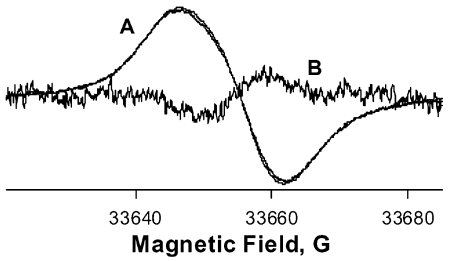

Figure 4. Oxygen effect on the $m_I = {}^1/_2$ component of a 95 GHz CW EPR spectrum from a 0.75 mM solution of Con-A in pH 6.4 HEPES: (A) superimposed intensity-normalized signals from oxygen- and helium-equilibrated samples at 3 atm of pressure and (B) 5-fold-increased residual of the fit to eq 1 but assuming that there is no change in the linewidth.

metalloprotein site, we have examined the Mn^{2+} center in Con-A lectin from *Canavalia ensiformis*. The manganese binding site is located in a crevice near the surface of the protein created by the conjunction of several loops.[25−27] Figure 4A shows experimental intensity-normalized W-band EPR spectra from oxygen- and helium-equilibrated pH 6.4 HEPES 0.75 mM solutions of Con-A at 3 atm of pressure of each gas. Under these conditions, the oxygen effect was 170 ± 30 mG, as determined from a least-squares fit to eq 1. Figure 4B shows the 5-fold-magnified residual of this fit (the difference between experimental and simulated spectra, assuming that there is no change in the line width; i.e., the position, baseline line, and dispersion contributions vary, but the linewidth was not allowed to vary). The plot of square symbols in Figure 3 shows the pressure dependence of oxygen broadening for the Con-A Mn^{2+} center. Although the oxygen broadening at 1 atm is only 53 ± 30 mG, which is the limit of detection, the pressure dependence shows that, at elevated pressures, the effect is measured easily and reliably.

To demonstrate that oxygen accessibility to the Mn^{2+} center in Con-A changes with modifications in the metal coordination, we fully denatured Con-A in 4 M guanidine hydrochloride (GndHCl). The room-temperature 95 GHz EPR spectrum from the Mn^{2+} center changed drastically, reflecting the release of Mn^{2+} ions into the GndHCl solution. Oxygen broadening observed at 1 atm of pressure for the Mn^{2+} center in denatured protein was 180 ± 30 mG, which is very similar to that of the aqua ion.

Conclusions

We have demonstrated initial experiments to directly observe dynamic magnetic interactions between Mn^{2+} ions and molecular oxygen (O_2) in solutions from linewidth effects on high-

field (95 GHz, 3.4 T, W-band) electron paramagnetic resonance (EPR) spectra. These experiments show that the effect of O_2 on continuous-wave (CW) EPR spectra from aqueous Mn^{2+} complexes can be described as an additional Lorentzian broadening whose magnitude is independent of the frequency of the EPR experiment but changes with the oxygen permeability coefficient of the solvent. The observed effect is likely to be caused by Heisenberg exchange between electronic spins of oxygen and the Mn^{2+} ion during bimolecular collisions. A very interesting observation is that the O_2 effect on Mn^{2+} CW EPR spectra is dependent on the immediate microenvironment of the ion. More experiments are necessary to determine how the magnitude of the effect is related to the structure of the ion complex in solution. We have demonstrated the feasibility of O_2 accessibility experiments for Mn^{2+} centers in proteins at elevated oxygen pressures. It is hypothesized that O_2 accessibility experiments provide a measure of the dynamic properties of the metal ion coordination. After this method has been developed further, it would complement the rich, but static, structural information obtained from electron paramagnetic resonance/electron spin echo envelope modulation/electron nuclear double resonance (EPR/ESEEM/ENDOR) experiments with frozen Mn^{2+}-containing protein samples.

Acknowledgment. This work was supported by a grant from the National Science Foundation (No. MCB-0196326) (T.I.S.) and used W-band (95 GHz) facilities of the Illinois EPR Research Center (IERC), which are supported by the National Institutes of Health (under Contract No. R01-RR01811).

References and Notes

(1) Meuwly, M.; Becker, O. M.; Stote, R.; Karplus, M. *Biophys. Chem.* **2002**, *98*, 183.
(2) Lakowicz, J. R.; Weber, G. *Biochemistry* **1973**, *12*, (21), 4161.
(3) Lakowicz, J. R.; Weber, G. *Biochemistry* **1973**, *12*, (21), 4171.
(4) Teng, C. L; Bryant, R. G. *J. Am. Chem. Soc.* **2000**, *122*, (11), 2667.
(5) Prosser, R. S.; Luchette, P. A.; Westerman, P. W.; Rozek, A.; Hancock, R. *Biophys. J.* **2001**, *80*, (3), 1406.
(6) Luchette, P. A.; Prosser, R. S.; Sanders, C. R. *J. Am. Chem. Soc.* **2002**, *124*, (8), 1778.
(7) Altenbach, C.; Marti, T.; Khorana, H. G.; Hubbell, W. L. *Science* **1990**, *248*, (4959), 1088.
(8) Klug, C. S.; Su, W.; Feix, J. B. *Biochemistry* **1997**, *36*, (42), 13027.
(9) Feix, J. B.; Klug, C. S. In *Spin Labeling: The Next Millennium*; Berliner, L. J., Ed.; Biological Magnetic Resonance 14; Plenum Press: New York, 1996; pp 251−281.
(10) Altenbach, C.; Flitsch, S. L.; Khorana, H. B.; Hubbell, W. L. *Biochemistry* **1989**, *28*, 7806.
(11) Hubbell, W. L.; Altenbach, C. *Curr. Opin. Struct. Biol.* **1994**, *4*, 566.
(12) Hyde, J. S.; Subczynski, W. K. In *Spin Labeling: Theory and Applications*; Berliner, L. J., Reuben, J., Eds.; Biological Magnetic Resonance 8; Plenum Press: New York, 1989; p 399.
(13) Ashikawa, I.; Yin, J.-J.; Subczynski, W. K.; Kouyama, T.; Hyde, J. S.; Kusumi, A. *Biochemistry* **1994**, 33, 4947.
(14) Lai, C.-H.; Hopwood, L. E.; Hyde, J. S.; Lukiewicz, S. *Proc. Natl. Acad. Sci. U.S.A.* **1982**, *79*, 1166.
(15) Rosen, G. M.; Halpern, H. J.; Brunsting, L. A.; Spencer, D. P.; Strauss, K. E.; Bowman, M. K. *Proc. Natl. Acad. Sci. U.S.A.* **1988**, *85*, 7772.
(16) Likhtenshtein, G. I. *Biophysical Labeling Methods in Molecular Biology*; Cambridge University Press: New York, 1993; pp 70−71.
(17) Subczynski, W. K.; Hyde, J. S.; Kusumi, A. *Proc. Natl. Acad. Sci. U.S.A.* **1989**, *86*, 4474.
(18) Smirnov, A. I.; Clarkson, R. B.; Belford, R. L. *J. Magn. Reson. B* **1996**, *111*, 149.
(19) Altenbach, C.; Marti, T.; Khorana, H. G.; Hubbell, W. L. *Science* **1990**, *248*, 1088.
(20) Yu, J.-S.; Kim, J. Y.; Kevan, L. *Microporous Mesoporous Mater.* **2000**, *40*, 135−247.
(21) Sigel, A.; Sigel, H. *Manganese and Its Role in Biological Processes*; Metal Ions in Biological Systems 37; Marcel Dekker: New York, 2000, 761 p.
(22) Smirnova, T. I.; Smirnov, A. I.; Clarkson, R. B.; Belford, R. L. *Magn. Reson. Med.* **1995**, *33*, (6), 801.
(23) Smirnov, A. I.; Belford, R. L. *J. Magn. Reson., Ser. A* **1995**, *113*, 65−73.
(24) Smirnov, A. I.; Norby, S. W.; Weyhenmeyer, J. A.; Clarkson, R. B. *Biochem. Biophys. Acta* **1994**, *1200*, 205.
(25) Deacon, A.; Gleichmann, T.; Kalb, A. J.; Price, H.; Raftery, J.; Bradbrook, G.; Yariv, J.; Helliwell, J. R. *J. Chem. Soc.—Faraday Trans.* **1997**, *93*, 4305.
(26) Bouckaert, J.; Loris, R.; Wyns, L. *Acta Crystallogr., Sect. D: Biol. Crystallogr.* **2000**, *D56*, 1569.
(27) Shoham, M.; Kalb, A. J.; Pecht, I. *Biochemistry* **1973**, *12*, 1914.